A Self-Adaptive AP Selection Algorithm Based on Multiobjective Optimization for Indoor WiFi Positioning

Wei Zhang, *Member, IEEE*, Kegen Yu, *Senior Member, IEEE*, Weixi Wang, and Xiaoming Li, *Member, IEEE*

***Abstract*—With the widely deployed wireless access points (APs) and the worldwide popularization of smartphones, WiFi-based indoor positioning has attracted great attention to both industry and academia. Locating and tracking objects within an indoor environment plays an important role in Internet of Things application and service. However, it is a challenging problem to achieve high accuracy using WiFi positioning technique due to the high instability in received signal strength from AP. Thus, it is desirable to select APs by considering both signal strength and connection quality. In this article, an AP selection algorithm based on multiobjective optimization is proposed to improve indoor WiFi positioning accuracy. The self-adaptive AP selection algorithm can be easily applied to various real scenarios and the performance of the new method is considerably better than classical algorithms. Learning algorithm is exploited to obtain the optimal solution for the self-adaptive AP selection algorithm. Experiments are conducted and the proposed algorithm is compared with classical algorithms. The experimental results demonstrate that the performance of the self-adaptive AP selection algorithm is at least a few decimeters better than classical algorithms in terms of RMSE of position estimation. Meanwhile, the new method is robust to the random generation of initial particles and normalizing factor as their effect on the positional accuracy is less than 1 decimeter.**

***Index Terms*—Access point (AP) selection, indoor WiFi positioning, Internet of Things (IoT), multiobjective optimization, self-adaptive algorithm.**

I. Introduction

INDOOR positioning is used in various fields such as transportation [1], health care [2], [3], entertainment [4], [5], education [6], tourism [7], emergency [8], [9] and so on. The rapid growth of wireless communication technology and smart mobile device become major driving force behind the indoor positioning and the location-based service (LBS) [10]. The accurate and precise positioning technology is the foundation of numerous Internet of Things (IoT) applications and the accurate and precise location data is a key element in a comprehensive IoT solution [11]–[14]. Compared to GNSS technology for outdoor positioning [15], which has sufficient accuracy for most of outdoor IoT applications, indoor positioning still faces many practical challenges due to the complex indoor environments [16], [17].

Numerous technologies are investigated and developed for indoor positioning and navigation such as WiFi [18], [19], Bluetooth low energy (BLE) [20], [21], ultrasonic [22], camera [23] and so on. However, indoor positioning system (IPS) often does not work well in real scenarios due to the complex and the dynamically changing indoor environment [16], [24]. With the widely deployed WiFi infrastructures [25] and the popularization of smartphones [26], indoor WiFi positioning technology attracts a wide attention as it makes use of the existing network infrastructure. Location estimation based on received signal strength (RSS) is the prevalent method in indoor WiFi positioning [27]–[30]. Fingerprinting match and triangulation are two methods commonly used for position estimation. In order to improve WiFi IPS accuracy, usually an on-the-spot survey is needed for triangulation algorithm to determine the signal-attenuation models [31]. However, it is difficult to distinguish signal attenuation caused by distance and that by environmental factors from each other without sufficient prior information. A self-adaptive indoor WiFi localization method based on triangulation is proposed in [32], but its performance will degrade without the information about access points (APs) and walls. In general, fingerprinting match has a better performance in terms of accuracy and precision than RSS-based triangulation algorithm. Most of the WiFi IPSs make use of the fingerprinting technique which has two main phases: offline phase and online phase [33], [34]. A database consisting of the positions over the positioning area and the corresponding RSSs is constructed in the offline phase. In the online positioning phase, at each sampling time instant, corresponding to a specific target position, an RSS vector is observed by the mobile device and the

Manuscript received March 16, 2020; revised May 10, 2020; accepted July 20, 2020. Date of publication July 23, 2020; date of current version January 22, 2021. This work was supported in part by the Natural Science Foundation of Shandong Province under Project ZR2014EEM025; in part by the China 973 Program under Grant 2013CB228305; in part by the China National Nature Science Foundation of China under Grant 61402047, Grant 61511130081, and Grant 61273217; in part by the National Key Research and Development Program of China under Grant 2016YFB0502102; in part by the Natural Science Foundation of Guangdong Province under Grant 2019A1515010748 and Grant 2019A1515011872; and in part by the National Nature Science Foundation of China under Grant 41971341 and Grant 41971354. *(Corresponding authors: Wei Zhang; Weixi Wang.)*

Wei Zhang is with the Research Institute for Smart Cities, Shenzhen University, Shenzhen 518060, China (e-mail: weizhsz@szu.edu.cn).

Kegen Yu is with the School of Environmental Science and Spatial Informatics, China University of Mining and Technology, Xuzhou 221116, China (e-mail: kegen.yu@cumt.edu.cn).

Weixi Wang and Xiaoming Li are with the School of Architecture and Urban Planning, Shenzhen University, Shenzhen 518060, China (e-mail: wangwx@szu.edu.cn; lixming@szu.edu.cn).

Digital Object Identifier 10.1109/JIOT.2020.3011402

observed RSS vector is compared with each of the components or fingerprints in the database, followed by position determination.

Although there have been many previous studies on WiFi IPS based on RSS. The AP selection criterion [35] is still confused and the empirical parameters of the AP selection model are hardly universally suitable. The existing AP selection criteria may be classified in two types: offline AP selection criteria and online AP selection criteria. The general offline AP selection criteria use information gain (IG) and joint information gain [36]–[38], whereas typical online AP selection criteria use max mean RSS [36], loss rate and mutual information [39]. The performance of AP selection criterion-based loss rate is affected by the loss rate threshold, which has to be determined by field test. The rest criteria need to carefully choose the number of selected APs. A self-adaptive WLAN AP for optimizing network performance using multiobjective genetic algorithm (GA) is proposed in [40], which intends to make the AP adaptive to interference and link quality of client stations. However, the algorithm cannot be used directly in WiFi IPS because it is suited for improving the AP performance but not for selecting AP for the WiFi positioning.

This article proposed a self-adaptive AP selection algorithm based on multiobjective optimization for WiFi IPS, which does not involve any empirical parameter. The number of APs used by Max MEAN (MM) RSS-based AP selection algorithm and the loss rate threshold used by loss rate (LR)-based AP selection algorithm can perform automatic regulation in the new algorithm, which reduce some field test work. The major contributions of this article are summarized as follows.

1) We propose a robust self-adaptive AP selection algorithm for indoor WiFi positioning. Our AP selection algorithm does not involve any empirical parameter, which avoids the effect of empirical parameter for the existing AP selection algorithms. The proposed method achieves improved accuracy for static indoor WiFi positioning, which is suitable to asset tracking and generation of accurate initial WiFi indoor location and so on.
2) We have developed GA and particle swarm optimization (PSO) mathematical formulation to solve the multiobjective optimization problem. It is the first time to prove the feasibility of using self-adaptive AP selection for indoor WiFi positioning. The proposed algorithms are robust to the random generation of initial particles and variation of normalizing factor.

The remainder of this article is organized into 4 sections as follows. In Section II, we briefly summarize existing works on the AP selection algorithms for IPSs. The GA and PSO algorithm are described and used to obtain the optimal solution for the self-adaptive AP selection algorithm with details given in Section III. Experiments have been conducted to evaluate the performance of the proposed AP selection algorithm and the results are presented in Section IV. Finally, Section V concludes the findings of this article.

II. AP Selection Strategies

As mentioned earlier, a number of different AP selection strategies have been proposed in the literature. The purpose of each AP selection strategy is to select a subset of APs from all available APs, and only the selected subset of APs is used to estimate target position, whereas other APs are excluded. Details of the five mentioned selection strategies are provided below.

A. AP Selection Algorithm Based on the Max MEAN RSS

RSS observation sequence associated with an AP typically fluctuates over time due to the dynamic indoor environment. Based on the assumption that a location closer to the AP will have a higher RSS value, the MM RSS-based AP selection strategy selects N APs with the largest mean RSS. Although the MM AP selection strategy can achieve acceptable results at most times, the number of subset APs needs to be chosen carefully, which is usually determined through field survey. Ideally, each AP can contribute to fingerprinting feature, which means the more APs, the better positioning accuracy.

B. AP Selection Algorithm Based on the Loss Rate

Intuitively, we should choose the APs that appear most of the time in the RSS samples. This is the basis for the AP selection algorithm based on the LR; the APs with a LR lower than a threshold of loss rate are selected. The LR-based algorithm can be summarized as follows.

1) At the target location, the device carried by the target scans the wireless channel n times and records RSS observations of all available APs each time.
2) Count the number of RSS observations related to each AP.
3) Calculate the loss rate of each AP according to

$$LR_i = (n - n_i)/n. \tag{1}$$

Here, i denotes the ith AP, LR_i denotes the loss rate which is between 0 and 1, and n_i is the number of RSS observations of the ith AP over the n-time scanning.

Select the APs which have loss rates smaller than the loss rate threshold. Generally, a smaller loss rate threshold will reduce the number of selected APs. Therefore, in order to ensure the positioning accuracy, the loss rate threshold should not be too small.

C. AP Selection Algorithm Based on the Mutual Information

The mutual information (MI) between each pair of APs is utilized by the MI minimization-based AP selection strategy, which uses MI as a measure of the independence between APs. The greater the MI is, the more redundant information is included in the selected subset of AP, while the smaller the MI is, the smaller the correlation between the selected APs is and the stronger collective discrimination ability is obtainable. Zou *et al.* [41] described the detailed process of AP selection based on MI minimization.

D. AP Selection Algorithm Based on the Information Gain

An AP selection based on IG was proposed by Chen *et al.* [42] to found a tradeoff point between the number of APs used and the accuracy they can achieve. Each AP is viewed as a location information source, and the RSS sample received from this AP at reference point can provide some location information. The discriminant ability of each AP is measured independently in IG-based AP selection algorithm, and the IG of each AP is calculated by

$$IG(AP_i) = H(L) - H(L|AP_i). \tag{2}$$

Here, $IG(AP_i)$ is the IG of the ith AP, $H(L)$ stands for the information entropy of calibration point or reference point, and $H(L|AP_i)$ is the conditional entropy of the calibration point when giving the information from the ith AP. Giving *a priori* conditional probability, they can be calculated by

$$\begin{aligned} H(L) &= -\sum_{j=1}^{n} P(l_j)\log(P(l_j)) \\ H(L|AP_i) &= -\sum_{\{v_i\}}\sum_{j=1}^{n} P(l_j, AP_i = v_i)\log(P(l_j|AP_i = v_i)). \end{aligned} \tag{3}$$

Here, $P(l_j)$ is the probability of calibration point, which can be assumed to be equally in any reference point. $\{v_i\}$ are the set of distinct RSS values of the ith AP detected at the jth calibration point. $P(l_j|AP_i = v_i)$ is the conditional probability which can be computed by

$$P(l_j|AP_i = v_i) = P(AP_i = v_i|l_j) \cdot P(l_j)/P(AP_i = v_i). \tag{4}$$

Then, N APs with maximum IG are selected for online localization process.

E. AP Selection Algorithm Based on the Joint Information Gain

The joint IG (JIG) maximization-based AP selection strategy, which measures the discriminant ability of subset of APs, selects the subset of APs with maximum JIG. Suppose that a subset of N APs $(AP_1, AP_1, \ldots, AP_N)$ are used for positioning and there are totally n detectable APs, and hence there are totally C_n^N combinations of subsets of APs. The joint location IG of the combination of arbitrarily N APs is defined as [43]

$$\begin{aligned} JIG(AP_1, AP_2, \ldots, AP_N) &= H(L) \\ &\quad - H(L|AP_1, AP_2, \ldots, AP_N). \end{aligned} \tag{5}$$

Here, $JIG(AP_1, AP_1, \ldots, AP_N)$ is the JIG of the N APs, and the combination with max JIG is selected, and then the N APs are used for online localization process. $H(L|AP_1, AP_1, \ldots, AP_N)$ is the conditional entropy of the calibration point when giving the information from N APs, which can be calculated as follows:

$$\begin{aligned} H(L|AP_1, \ldots, AP_N) = -\sum_{\{v_i\}}\sum_{j=1}^{n} & P(l_j, AP_1, \ldots, AP_N = \mathbf{v}_i) \\ & \times \log(P(l_j|AP_1, \ldots, AP_N = \mathbf{v}_i)). \end{aligned} \tag{6}$$

Here, N denotes the number of subset APs, $\{\mathbf{v}_i\}$ is the set of distinct RSS vector of the subset APs detected at the jth calibration point, and $P(l_j|AP_1, \ldots, AP_N = \mathbf{v}_i)$ is the conditional probability.

III. Self-Adaptive AP Selection Algorithm Based on Multiobjective Optimization

Compared to the AP selection algorithms performed at offline phase, the proposed AP selection algorithm based on multiobjective optimization is an online-phase AP selection algorithm. The main disadvantage of offline selection is that some selected APs may not be suited at the online phase. The two schemes of MM and LR intend to select APs close to the positioning area of interest so as to obtain stronger RSS and better connection quality. The computational complexity of the two schemes is a linear function of the number of APs that are detected at the target point. Thus, the selection of the two schemes is for consideration of both low computational complexity and good positional accuracy. The main purpose for fusing MM and LR schemes is to obtain more suited APs so that the positioning accuracy can be enhanced.

Assume that there are two separate subsets of APs selected by the MM-based AP selection algorithm and the LR-based AP selection algorithm, which are represented by $\{AP_i\}_{MM}$ and $\{AP_i\}_{LR}$, respectively. The multiobjective fitness function f is defined as

$$f = (n_U - n_I)/n_U \tag{7}$$

where, n_U is the number of APs in the union of the two subset of APs, and n_I is the number of APs in the intersect of the two subset of APs.

It can be easily seen from (7) that the fitness function f is equal to 0 when the two AP selection algorithms select the same subset of APs. On the other hand, if the selected two subset of APs are completely different, then the fitness function is equal to 1. Thus, f is an index that measures the AP consistency of the MM-based AP selection algorithm and LR-based AP selection algorithm.

As discussed in the preceding section, the MM-based AP selection algorithm is affected by the number of the subset of APs, which is specified empirically. The AP selection algorithm based on the LR is affected by the loss rate threshold. The number of subset APs and the loss rate threshold are usually determined through field survey, which usually cannot be used in different environments. Therefore, a novel self-adaptive AP selection algorithm based on multiobjective optimization is proposed to determine the number of the subset of APs and the loss rate threshold automatically. There are two main steps in the self-adaptive AP selection algorithm.

At the first step, the number of the subset of APs and the loss rate threshold are automatically regulated through the learning algorithm in order to obtain the minimum fitness function.

At the second step, two subsets of APs are selected through the MM-based AP selection algorithm and the LR-based AP selection algorithm, respectively. The number of the subset of APs and the loss rate threshold determined at the first step are used. Then, the union of the two subsets of APs with minimum fitness function is selected by the multiobjective optimization

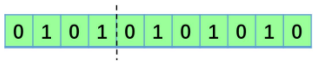

Fig. 1. Diagrammatic of chromosome.

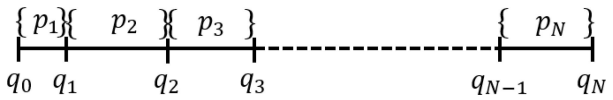

Fig. 2. Diagram of selection probability and cumulative probability. The length of each line segment equals a selection probability, and $q_i = \sum_{j=1}^{i} p_j$ is a positive number on the horizontal positive axis, which equals the cumulative probability up to the ith point.

as the final subset of APs and used to determine the location of target point. According to (7), the smaller fitness function f, most of the APs selected by the multiobjective optimization will simultaneously have both stronger signal strength and better connection quality.

In order to avoid the extreme situation where the selection algorithm selects too few APs or even no APs, a penalty factor is defined to select sufficient APs and the new multiobjective fitness function is defined as

$$f = 0.5 \cdot (n_U - n_I)/n_U + 0.5 \cdot |n_U - 10|/n_U. \tag{8}$$

Here, the normalizing factor of 0.5 is selected empirically and the selection has been tested by extensive experiments. $|\cdot|$ denotes the absolute value. Like the most fitness calculations, the normalizing factor makes the fitness value limited in the closed interval [0, 1] as far as possible. The fitness value calculated by (8) is always less than 1 except the case where n_U is less than 5, which rarely occurs due to the large numbers of existing APs in indoor environment. The normalizing factor also weighs the two items on both sides of the plus sign. Thus, the effect of the penalty factor in (8) can be allocated in a range by setting the reasonable normalizing factor.

Two learning algorithms are separately used to obtain the optimal solution of the multiobjective optimization problem, which are called GA and PSO. The performance comparison is also performed between the two learning algorithms in Section IV.

A. Multiobjective Optimization Based on GA

GA is a metaheuristic algorithm inspired by the process of natural selection that belongs to the larger class of evolutionary algorithms [44], [45]. There are six steps involved in multiobjective optimization based on GA.

1) Initialization: To solve this problem using GA, our first step is to define chromosomes that represent the individuals. Then, a population is randomly generated, which is composed of N different individuals. Each individual represents one case of the number of APs and loss rate threshold. Here, the chromosome is set to a binary string of 11 digits, among which the first 4 digits represent the number of APs and the remaining 7 digits represent the loss rate threshold, as illustrated in Fig. 1. Thus, the number of APs n and the loss rate threshold lr can be calculated as

$$\begin{aligned} &n = t_1 + 3 \\ &lr = t_2/100 \text{ if } lr > 0.99 \text{ set } lr = 0.99 \end{aligned} \tag{9}$$

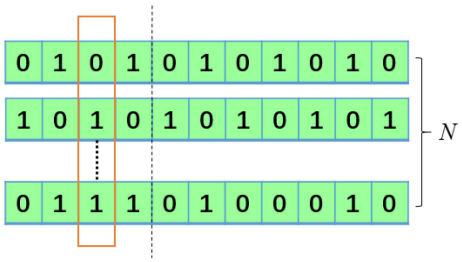

n_3^0 = the number of individuals which the third code is 0

$n_3^1 = N - n_3^0$

Fig. 3. Diagram about the process of $n_i^0$and n_i^1 calculation when the i is set to 3, and N is the number of individuals in the population.

where $t_1 (0 \le t_1 \le 15)$ is the corresponding decimal integers of the first 4 digits of the binary string, t_1 equals to 0 when all the binary digits are 0 and t_1 equals to 15 when all the binary digits are 1. $t_2 (0 \le t_2 \le 127)$ is the corresponding decimal integers of the last 7 digits of the binary string, t_2 equals to 0 when the all the binary digits are 0 and t_2 equals to 127 when all the binary digits are 1. An additive constant is used to make sure the number of APs n is no less than 3.

2) Fitness: The fitness f assigned to each individual after generating and initializing the population. First, the subset APs $\{AP_i\}_{MM}$ with n APs are selected by the MM-based AP selection algorithm, whereas the subset APs $\{AP_i\}_{LR}$ are selected by the LR-based AP selection algorithm with the loss rate threshold set to lr. The fitness value is calculated by the $\{AP_i\}_{MM}$ and $\{AP_i\}_{LR}$ according to (8).

3) Selection: After fitness assignment has been performed, the roulette wheel selection [46] is used to choose the individuals that will recombine for the next generation. Three steps are involved in roulette wheel selection implementation.

The first step is to calculate the selection probability p_i and the cumulative probability q_i of the ith individual according to

$$\begin{aligned} &p_i = (1 - f_i)/\sum_{i=1}^{N}(1 - f_i) \\ &q_i = \sum_{j=1}^{i} p_j \end{aligned} \qquad i = 1, 2, \ldots, N \tag{10}$$

where f_i is the multiobjective optimization function value of the ith individual, the smaller f_i, the higher selection probability, and N is the number of individuals. Fig. 2 illustrates the relationship between the selection probability and the cumulative probability.

The second step is to produce a random number $r (0 < r <= 1)$ and select the corresponding individual. If r is less than q_1, select the first individual, otherwise select the ith individual if r is less than q_i and greater than q_{i-1}.

At the third step, repeat the second step until N individuals are selected.

4) Mutation: The mutation operator is used to keep variety of population. The mutation rate is determined by the position of binary digit and the number of individuals that have the same binary digit at the position. Assume the $n_i^0 (i = 0, 1, \ldots, 11)$ is the number of individuals that the ith

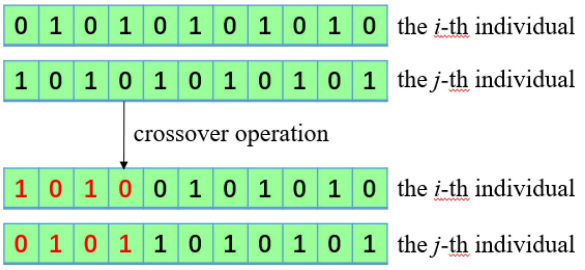

Fig. 4. Diagram of crossover operation between the ith individual and the jth individual.

binary digit is 0, whereas n_i^1 is the number of individuals that the ith binary digit is 1.

Then, the mutation of ith binary digit of the jth individual can be given as

$$\begin{aligned} p &= 1 - n_i^0/N \text{ if code is } 0 \\ p &= n_i^0/N \text{ if code is } 1 \end{aligned} \tag{11}$$

where N is the total number of individuals in the population. Produce a random number r and change the ith binary code of the jth individual if r is less than p. Fig. 3 illustrates the n_i^0 and n_i^1 calculation process when i is set to 3.

5) Crossover: The crossover operator is another method that is used to keep variety of population. Here, the number of times of crossover is set to $N/2$. At each crossover operation time, two individuals are randomly selected and the first 4 binary digits are exchanged. After $N/2$ times crossover operation, the new generated population is produced. Fig. 4 illustrates the example of crossover operation between two individuals.

6) Iteration: Repeat from 2) to 5) until the termination condition is satisfied.

B. Multiobjective Optimization Based on PSO

PSO was developed in 1995 by Kennedy and Eberhart [47], inspired by the behavior of social organisms in groups, such as bird and fish schooling or ant colonies. In PSO, every solution is entitled as a particle, and the combination of particles constitutes the whole swarm. In this article, the particle is in the form of vector of length 2. There are four steps involved in multiobjective optimization based on PSO.

1) Initialization: N particles are randomly produced at the initialization step, the ith particle x_i is represented as follows:

$$x_i = [n_i lr_i]^T \tag{12}$$

where, n_i denotes the number of APs selected by MM-based AP selection algorithm, whereas lr_i represents the loss rate threshold used by LR-based AP selection algorithm.

2) Fitness: All of the particles have fitness values f, which are calculated by the subset APs $\{AP_i\}_{MM}$ and the subset APs $\{AP_i\}_{LR}$. The $\{AP_i\}_{MM}$ with n_i APs are selected by the MM-based AP selection algorithm, whereas the $\{AP_i\}_{LR}$ are selected by the LR-based AP selection algorithm with the loss rate threshold set to lr_i.

Let f_i denotes the fitness value of current ith particle and f_i^{best} denotes the fitness value of the best ith particle in the history. If the f_i is less than f_i^{best}, then update the f_i^{best} and the best ith particle in the history x_i^{best} is given as follows:

$$\begin{aligned} x_i^{\text{best}} &= x_i \\ f_i^{\text{best}} &= f_i \end{aligned} \tag{13}$$

where x_i denotes the current ith particle.

3) Update Particle Velocity and Particle: Let x_g^{best} denote best particle in the current whole swarm, thus the particle velocity is given as follows:

$$\begin{aligned} v_i(t+1) &= w \cdot v_i(t) + c_1 \cdot r_1 \cdot \left(x_i^{\text{best}} - x_i(t)\right) \\ &\quad + c_2 \cdot r_2 \cdot \left(x_g^{\text{best}} - x_i(t)\right) \\ x_i(t+1) &= x_i(t) + v_i(t+1) \end{aligned} \tag{14}$$

where t denotes the iteration counts, $v_i(t+1)$ and $v_i(t)$ are the velocity of the ith particle, $x_i(t)$ and $x_i(t+1)$ are the ith particle before and after t times iteration. c_1 and c_2 are two positive constants, and both take the value 1. r_1 and $r_2$are random numbers generated by random function, and both r_1 and r_2 range from 0 to 1. w is the inertia weight which is calculated by the linearly decreasing weight [48]

$$w = (w_{\max} - w_{\min}) \cdot \frac{\text{Iter}N_{\max} - t}{\text{Iter}N_{\max}} + w_{\min}. \tag{15}$$

Here, inertia weight w linearly decreases from $w_{\max} = 0.9$ to $w_{\min} = 0.4$ through the search process [49], [50], $\text{Iter}N_{\max}$ is the maximum number of the allowed iterations.

4) Iteration: Repeat from 2) to 3) until the termination condition is satisfied.

Fig. 5. Picture of the laboratory rooms. Room 1 has the dimensions of 16.4 m × 7.5 m, Room 2 has the dimensions of 8.0 m × 7.5 m and Room 3 has the dimensions of 8.4 m × 7.5 m. A lot of desks have been arranged in the room 1 and room 3, whereas the Room 2 is relatively empty.

IV. Experiments and Performance Evaluation

A group of experiments have been conducted within three laboratory rooms, as shown in Fig. 5. There are over thirty students and staff members studying in the rooms, some of whom may walk in or walk out of the room from time to time.

Fig. 6 shows the layouts of calibration points and target points in the rooms. There are 235 target points denoted by

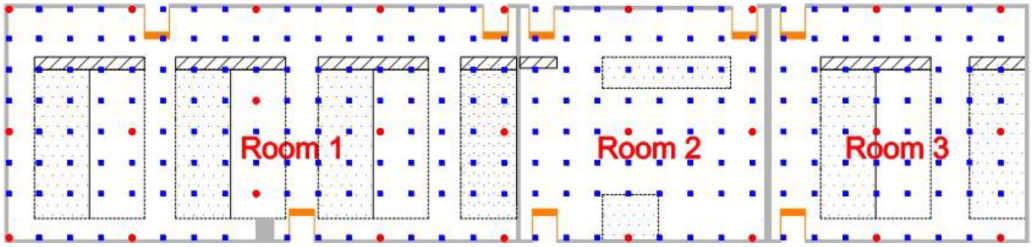

Fig. 6. Picture of the laboratory room. The rectangles with slash represent the bookcases, whereas the rectangles with dots represent the desks and sofa. There are three doors in the room 1 and room 2 and two doors in the room3, some of which may open or close from time to time.

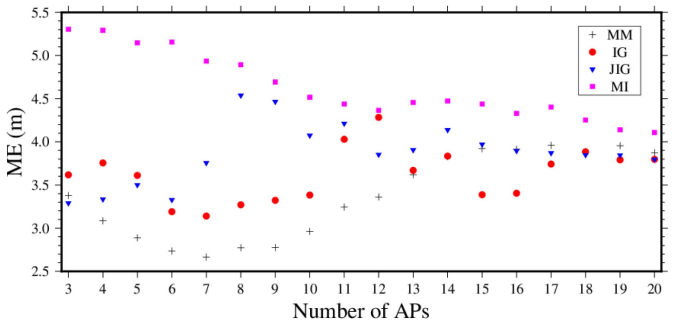

Fig. 7. Scatter diagrams of ME of four different AP selection algorithms with respect to the number of APs.

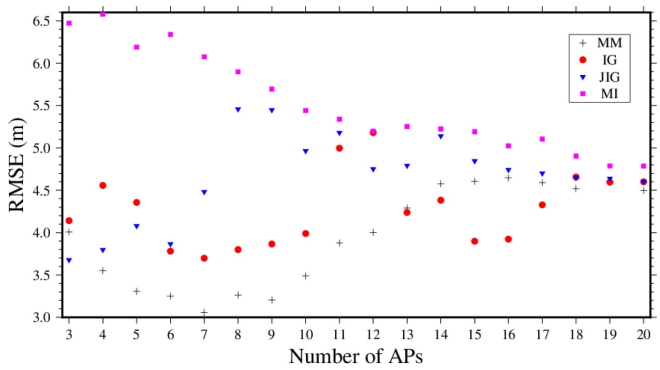

Fig. 8. Scatter diagrams of RMSE of four different AP selection algorithms with respect to the number of APs.

solid squares and 27 calibration points denoted by solid circles in the three rooms. The horizontal and vertical distance between two adjacent target points is about 1.0 m. In the experiment, a millet smart phone is used for receiving AP signals and all APs deployed in the building are treated as valid signal transmitters. A total of 120 Wi-Fi RSS samples are collected at each calibration point. As the scanning rate of Wi-Fi signal is 1 Hz, the scanning period of each target point is 2 min.

A. Analysis on the Effect of the Number of APs

To investigate the effect of the number of APs, eighteen different numbers (the integers from 3 to 20) of APs are tested. Figs. 7 and 8 show the scatter diagram of mean positioning error (ME) and root mean square error (RMSE) of the four different AP selection strategies. Weighted k nearest neighbor (WKNN) [51]–[53] algorithm is used to estimate the position of the target point, and k is set to 3 according to [54].

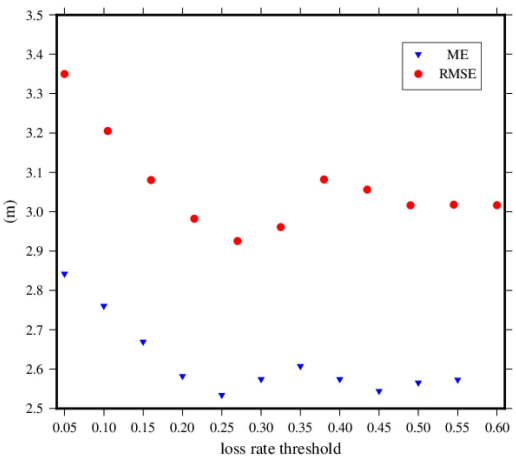

Fig. 9. Scatter diagrams of ME and RMSE of the AP selection strategy based on MI. The symbol inverted triangle is for the ME of the AP selection strategy based on LR, and the symbol circle is for the RMSE of the method.

Clearly, the accuracy of the positioning algorithm using any of the four AP selection strategies is affected by the choice of number of APs considerably.

In general, the MM-based AP selection algorithm can achieve the best accuracy, whereas the MI-based AP selection algorithm has the lowest accuracy. As the number of APs approaches 20, the accuracy difference among the four algorithms is marginal. There is no specific variation trend in accuracy with the increased number of APs. The best positioning accuracy was obtained by the MM-based AP selection algorithm with 7 APs.

B. Analysis on the Effect of the Loss Rate Threshold

The loss rate threshold ranges from 0.05 to 0.55 and the step size is 0.05. Fig. 9 shows how the ME and RMSE of the AP selection strategy based on LR change with the threshold.

It can be seen that the accuracy of the AP selection strategy based on LR is improved as the loss rate threshold increases from 0.05 to 0.25, which indicates the loss rate threshold should not be too small. The AP selection strategy based on LR obtains the minimum ME and RMSE when the loss rate threshold equals 0.25. Moreover, the ME and RMSE slightly change when the loss rate threshold goes from 0.25 to 0.55.

C. Performance Comparison Among Different AP Selection Strategies

Table I shows the positional accuracy in terms of three different indexes, and the online device-dependent execution time

TABLE I
PERFORMANCE FOR DIFFERENT AP SELECTION ALGORITHMS

AP selection algorithm	Empirical parameter	Parameter value	ME (m)	RMSE (m)	Standard deviation of positioning error (m)	Time (ms)
MM based AP selection	the number of APs	7	2.66	3.06	1.5019	0.017
		17	3.96	4.59	2.3223	0.004
IG based AP selection	the number of APs	7	3.14	3.70	1.9552	0.000
		12	4.28	5.18	2.9197	0.000
JIG based AP selection	the number of APs	3	3.29	3.68	1.6488	0.000
		8	4.54	5.46	3.0407	0.000
MI based AP selection	the number of APs	20	4.11	4.78	2.4584	52.243
		3	5.30	6.47	3.7174	17.249
LR based AP selection	the loss rate threshold	0.25	2.53	2.93	1.4647	0.004
		0.05	2.84	3.35	1.7770	0.003
ELM	-	-	6.44	7.64	4.1191	0.000
multi-objective optimization + GA	-	-	2.48	2.85	1.4138	49.244
multi-objective optimization + PSO	-	-	2.45	2.82	1.4119	4.130

The GA represents the self-adaptive AP selection algorithm based on multi-objective optimization and GA is used to obtain the optimal solution, whereas PSO represents the self-adaptive AP selection algorithm based on multi-objective optimization and PSO is used to obtain the optimal solution. The two representative parameter values of the existing AP selection algorithms are determined by the additional experiments, which represent the best case and the worst case of the corresponding AP selection algorithm. The hyphen "-" means that there is no empirical parameter need to determine in the AP selection model. All APs detected at the target point are used in the ELM.

TABLE II
RESULTS OF KOLMOGOROV–SMIRNOV HYPOTHESIS TEST

Average (m)	Standard deviation (m)	Max (m)	Min (m)	Alpha	p-Value	H
2.46	0.0177	2.51	2.41	0.05	0.6748	0

Average, standard deviation, max and min are the statistical characteristics of mean positioning error m_i $(1 \le i \le 1000)$. Alpha is the significance level. H equals 0 indicates that do not reject the null hypothesis at the 5% significance level.

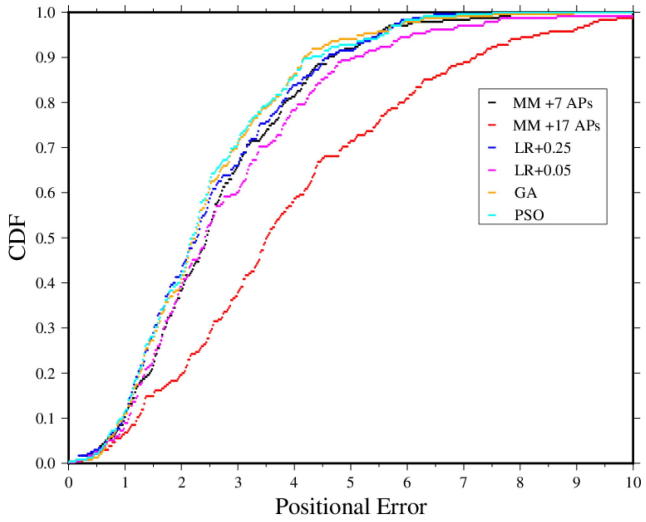

Fig. 10. CDF curves of different AP selection strategies. MM represents the AP selection algorithm based on MM, and the 7 APs and 17 APs means the number of APs selected by the AP selection algorithm. LR represents the AP selection algorithm based on LR, and 0.25 and 0.05 means the corresponding limiting loss rate. GA represents the self-adaptive AP selection algorithm based on multiobjective optimization and GA is used to obtain the optimal solution, whereas PSO means PSO is used to obtain the optimal solution.

caused by online AP selection. Without loss of generality, the population size of GA is set to 200 and the particle swarm size is also set to 200. The number of crossover operation of GA is set at 100 and the Iter$N_{\max}$ of PSO is also 100. The best case and the worst case of the existing AP selection algorithms and the self-adaptive AP selection algorithm are compared with each other. The AP selection algorithm based on IG and that based on JIG are two offline AP selection algorithms, so their online device-dependent execution time caused is equal to 0ms. An extreme learning machine (ELM) method [51] is also compared with the proposed self-adaptive AP selection algorithm. The ELM algorithm-based indoor WiFi positioning contains two main steps. First, the RSS vector of each calibration point is extracted from fingerprint database, which is taken as the input of ELM regression model. Taking the known coordinates of calibration points as the output of ELM regression model, Python Extreme Learning Machine library is used to train the ELM regression model with the extracted RSS vector and known coordinates. Second, the coordinate of target point is predicted by the trained ELM regression model with the known RSS vector of target points. The default parameters of Python Extreme Learning Machine library are chosen for the ELM regression model.

In general, for the AP selection algorithms which are considerably affected by the number of selected APs, the ME and RMSE in the best case are about 1 m less than the worst case for each of the AP selection algorithms. As seen from Table I, although the ME and RMSE in the best case are close to the worst case of the LR-based AP selection algorithm, the difference is still about 0.3 m. The positioning accuracy of the existing AP selection algorithms in the two extreme situations shows that the empirical parameters should be chosen carefully.

Although there has no online computation burden for the IG-based AP selection algorithm and JIG-based AP selection algorithm, the positioning accuracy is lower than other AP selection algorithms except for the MI-based AP selection algorithm. It also can be seen that the positional accuracy of ELM is the worst among all the algorithms.

Generally, the positional accuracy of self-adaptive AP selection algorithm is the highest among all the AP selection algorithms and the ELM method. For the self-adaptive AP

TABLE III
RESULTS OF DIFFERENT NORMALIZING FACTOR TEST

Normalizing factor	Average (m)	Standard deviation (m)	Max (m)	Min (m)
0.3	2.49	0.0120	2.53	2.44
0.35	2.48	0.0142	2.53	2.44
0.4	2.48	0.0141	2.53	2.44
0.45	2.46	0.0185	2.53	2.42
0.5	2.46	0.0177	2.51	2.41
0.55	2.46	0.0188	2.52	2.40
0.6	2.47	0.0218	2.54	2.41
0.65	2.49	0.0241	2.56	2.41
0.7	2.51	0.0228	2.60	2.45

Average, max and min represent the mean, maximum value and minimum value of 1000 mean positioning errors with the different normalizing factor.

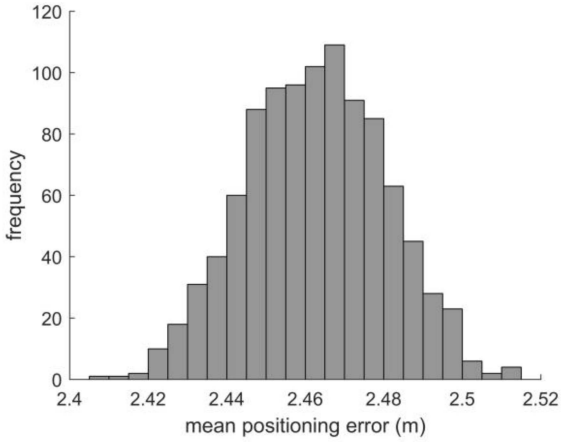

Fig. 11. Histogram of the mean positioning errors of 1000 position estimations. Frequency represents the number of occurrences of corresponding mean positioning error over each error bin.

selection algorithm based on multiobjective optimization, the performance of the GA-based scheme is close to the PSO-based scheme, whereas the execution time of the method with PSO is about 10 times of the method with GA. In a summary, the positioning accuracy of the multiobjective optimization based on PSO is the highest among all the AP selection algorithms. Although the execution time of PSO-based scheme is longer than the scheme with LR-based AP selection algorithm, it is acceptable for many IOT applications, such as robot navigation, advertising push and asset tracking.

Fig. 10 shows the cumulative distribution function (CDF) of the four AP selection strategies, including the MM-based AP selection algorithm, the LR-based AP selection algorithm and the two self-adaptive AP selection algorithms. The CDF curve of AP selection algorithm based on MM with 17 APs is below the other curves almost over the whole range, which indicates it has the worst positioning accuracy. Although CDFs for errors within 1 m of the GA and PSO are similar to those of the MM and LR algorithms, CDFs of the GA and PSO methods are significantly higher than those of the other approaches in the range of errors from 2.5m to 5.0m. In general, self-adaptive AP selection algorithm based on multiobjective optimization

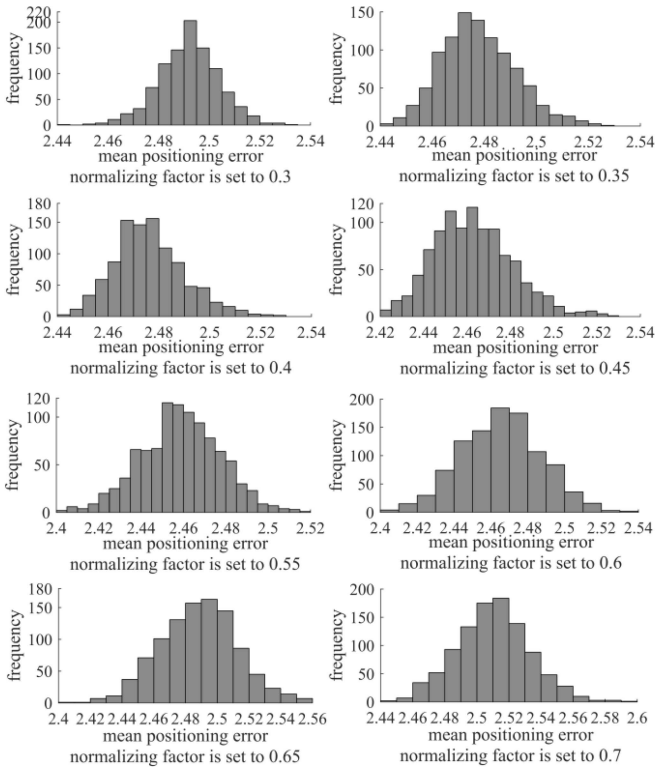

Fig. 12. Histogram of the mean positioning errors of 1000 position estimations with the different normalizing factors.

TABLE IV
RESULTS OF DIFFERENT K VALUE TEST

k	Average (m)	Standard deviation (m)	Max (m)	Min (m)
3	2.46	0.0174	2.51	2.42
4	2.43	0.0124	2.48	2.40
5	2.51	0.0127	2.57	2.44
6	2.64	0.0118	2.70	2.61
7	2.72	0.0123	2.77	2.68
8	2.77	0.0108	2.81	2.73
9	2.80	0.0113	2.83	2.76
10	2.79	0.0116	2.84	2.76

Average, max and min represent the mean, maximum value and minimum value of 1000 mean positioning errors with the different k value.

has a higher accuracy than the MM-based AP selection algorithm and LR-based AP selection algorithm. The self-adaptive AP selection algorithm based on multiobjective optimization with GA has the similar curve in almost the whole range of error to the self-adaptive AP selection algorithm based on multiobjective optimization with PSO.

D. Algorithm Robust Analysis

In order to analyze the effect of random generation of particles, 1000 experiments of self-adaptive AP selection algorithm based on multiobjective optimization and PSO are conducted. Let $m_i (1 \leq i \leq 1000)$ denotes the mean positioning error of the 235 target points at the ith experiment.

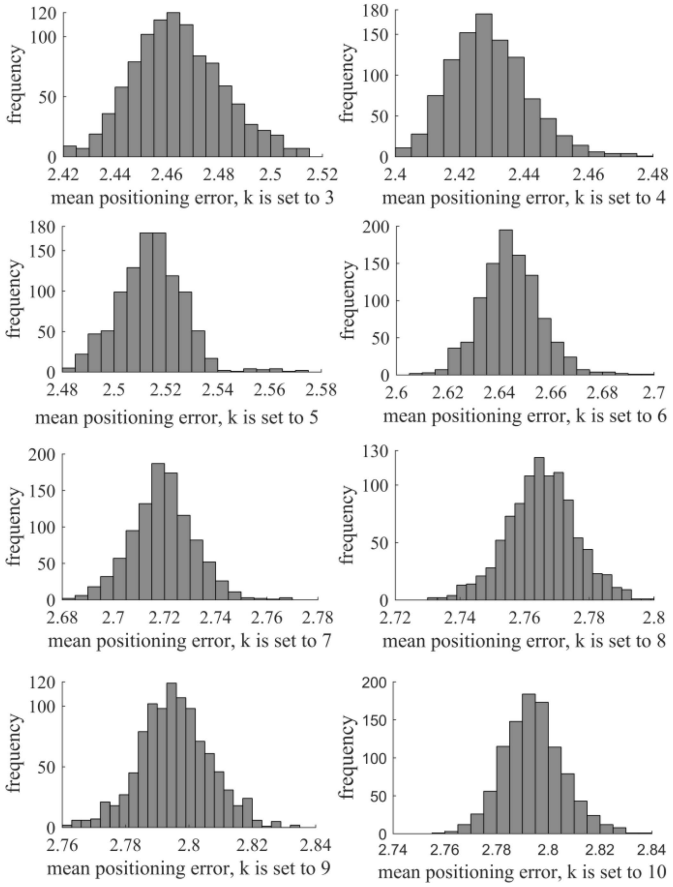

Fig. 13. Histograms of the 1000 mean positioning errors with the different k value.

Fig. 11 shows histogram of the 1000 mean positioning errors and Table II shows the results of Kolmogorov–Smirnov (KS) hypothesis test at the significance level 0.05. The KS test results show that the mean positioning error approximately obeys a standard normal distribution. It also can be seen that the max value of m_i is about 0.1 m bigger than the min value, which means the positional accuracy of self-adaptive AP selection algorithm based on multiobjective optimization and PSO is robust to the randomly generated initial particles. Even for the worst case of the 1000 replicated experiments, the positional accuracy of self- adaptive AP selection algorithm is the highest among all the AP selection algorithms and the ELM method, which are listed in Table I.

Furthermore, eight groups of experiments are conducted for the self-adaptive AP selection algorithm based on multiobjective optimization and PSO to analyze the effect of the normalizing factor in (8). The normalizing factor is set to 0.3, 0.35, 0.4, 0.45, 0.55, 0.6, 0.65 and 0.7, and 1000 replicated experiments are conducted for each specified normalizing factor. The histograms of the sets of 1000 mean positioning errors are shown in Fig. 12 and Table III shows the statistical characteristics. As shown in the histogram and Table III, the maximum difference in the mean positional errors between the nine different normalizing factors is just five centimeters, and all the standard deviations of the positional errors are rather small, only about one or two centimeters. This means the positional accuracy of self-adaptive AP selection algorithm based on multiobjective optimization and PSO is robust to the selection of normalizing factor.

E. K Value Effect Analysis

To investigate the effect of the value of k, eight different values (the integers from 3 to 10) of k are tested in 1000 replicated experiments. At each experiment, the APs are selected by self-adaptive AP selection algorithm based on multiobjective optimization and PSO, then different k value is set to estimate the positions of 235 target points, respectively. The histograms of the 1000 mean positioning errors with different k value are shown in Fig. 13. Table IV shows the statistical characteristics. As can be seen, the average positioning error would increase as k increases from 4 to 8. It also suggests that, in order to achieve the best accuracy, it is better to choose the value of k less than 5. The results also show that the proposed method can achieve good positional accuracy when k is set to be 3 or 4. Since the positional accuracy is very similar for k being 3 and 4, k is simply set to be 3.

V. Conclusion

The research and development of IoT technology and IoT application is practically changing the way people live. The indoor scenario is a primary and indispensable scenario for IoT applications due to the fact that people spend more than 80% of time indoors. The IoT benefits greatly not only from highly sophisticated and highly sensitive sensors, but also from other related technologies, such as artificial intelligence technology, big data technology, and indoor positioning technology and so on.

The pervasive adoption of WiFi in indoor environments has provided an opportunity to develop IPS that will not require investing in manufacturing or purchasing dedicated hardware. Wireless communication channels in indoor environments are usually rather noisy, causing the significant variation in RSS due to the multipath effect and complex signal propagation. AP selection is one of the important steps, which greatly affects the performance of indoor WiFi positioning. However, the existing AP selection algorithms need to choose the model parameters, which usually have to be determined by field survey. Thus, a self-adaptive AP selection algorithm based on multiobjective optimization for WiFi indoor positioning has been proposed in this article. Experiments were conducted and the results show that the proposed AP selection algorithm outperforms the other five popular AP selection algorithms in terms of accuracy. Moreover, online device-dependent execution time caused by AP selection indicates that the PSO algorithm is more efficient than the GA algorithm to obtain the solution of multiobjective optimization. The experimental results indicate that the new method is robust to both the random generation of initial particles and the normalizing factor. Also, the new method can achieves good performance when k is set to 3 or 4.

In general, the self-adaptive AP selection algorithm based on multiobjective optimization and PSO avoids the parameter selection problem of existing AP selection algorithm.

Although the execution time caused by AP selection is longer than LR-based AP selection algorithm, it is acceptable and many applications can still benefit from the new AP selection to obtain a better accuracy. It is worth mentioning that many new smartphones have a much lower scanning frequency of WiFi such as 3∼4 s for a single scanning due to the constraint imposed by Google. In such a low scanning circumstance, the performance of the proposed method and many other algorithms will be affected considerably. Thus, it is useful to do more investigations on WiFi positioning with scanning frequencies much lower than 1Hz in the future. More research will be conducted to further improve the performance of the indoor WiFi positioning that based on the new AP selection algorithm.

REFERENCES

[1] A. Wessels, X. Wang, R. Laur, and W. Lang, "Dynamic indoor localization using multilateration with RSSI in wireless sensor networks for transport logistics," *Procedia Eng.*, vol. 5, pp. 220–223, Sep. 2010.

[2] T. V. Haute *et al.*, "Performance analysis of multiple indoor positioning systems in a healthcare environment," *Int. J. Health Geograph.*, vol. 15, no. 1, p. 7, Feb. 2016.

[3] E. I. Konstantinidis *et al.*, "IoT of active and healthy ageing: Cases from indoor location analytics in the wild," *Health Technol.*, vol. 7, no. 1, pp. 41–49, Mar. 2017.

[4] M. Aravindan, G. Yamuna, and V. R. Ravindra, "Indoor localization based on wireless local area network fingerprint technique," *J. Comput. Theor. Nanosci.*, vol. 16, no. 4, pp. 1498–1501, Apr. 2019.

[5] D. Z.-Yazti, C. Laoudias, K. Georgiou, and G. Chatzimilioudis, "Internet-based indoor navigation services," *IEEE Internet Comput.*, vol. 21, no. 4, pp. 54–63, Jun. 2017.

[6] T. C. Huang, Y. Shu, T. C. Yeh, and P. Y. Zeng, "Get lost in the library? An innovative application of augmented reality and indoor positioning technologies," *Electron. Library*, vol. 34, no. 1, pp. 99–115, Feb. 2016.

[7] K. Shim, J. Yim, and J. Jeon, "Development of an indoor–outdoor positioning Android app for Anapji tourist guides," *Int. J. Softw. Eng. Appl.*, vol. 9, no. 3, pp. 195–208, Mar. 2015.

[8] X. Zhang, Y. Chen, L. Yu, W. Wang, and Q. Wu, "Three-dimensional modeling and indoor positioning for urban emergency response," *ISPRS Int. J. Geo Inf.*, vol. 6, no. 7, p. 214, Apr. 2017.

[9] C. Antoniou, V. Gikas, V. Papathanasopoulou, T. Mpimis, H. Perakis, and C. Kyriazis, "A framework for risk reduction for indoor parking facilities under constraints using positioning technologies," *Int. J. Disaster Risk Reduct.*, vol. 31, pp. 1166–1176, Oct. 2018.

[10] J. H. Hu and K. Seo, "An indoor location-based control system using Bluetooth beacons for IoT systems," *Sensors*, vol. 17, no. 12, p. 2917, Dec. 2017.

[11] A. C. J. Malar, G. Kousalya, and M. Ma, "Markovian model based indoor location tracking for Internet of Things (IoT) applications," *Clust. Comput.*, vol. 22, no. 5, pp. 11805–11812, Dec. 2017.

[12] S. Sadowski and P. Spachos, "RSSI-based indoor localization with the Internet of Things," *IEEE Access*, vol. 6, pp. 30149–30161, 2018.

[13] X. Lin *et al.*, "Positioning for the Internet of Things: A 3GPP perspective," *IEEE Commun. Mag.*, vol. 55, no. 12, pp. 179–185, Sep. 2017.

[14] S. Guo and J. Liu, "Guest editorial special issue on large-scale Internet of Things," *IEEE Internet Things J.*, vol. 3, no. 4, pp. 439–440, Jul. 2016.

[15] Z. Deng *et al.*, "Situation and development tendency of indoor positioning," *China Commun.*, vol. 10, no. 3, pp. 42–55, Apr. 2013.

[16] Q. Li, W. Li, W. Sun, J. Li, and Z. Liu, "Fingerprint and assistant nodes based Wi-Fi localization in complex indoor environment," *IEEE Access*, vol. 4, pp. 2993–3004, 2016.

[17] H. Zou, M. Jin, H. Jiang, L. Xie, and C. J. Spanos, "WinIPS: WiFi-based non-intrusive indoor positioning system with online radio map construction and adaptation," *IEEE Trans. Wireless Commun.*, vol. 16, no. 12, pp. 8118–8130, Oct. 2017.

[18] C. Yang and H. R. Shao, "WiFi-based indoor positioning," *IEEE Commun. Mag.*, vol. 53, no. 3, pp. 150–157, Mar. 2015.

[19] W. Xue, W. Qiu, X. Hua, and K. Yu, "Improved Wi-Fi RSSI measurement for indoor localization," *IEEE Sens. J.*, vol. 17, no. 7, pp. 2224–2230, Apr. 2017.

[20] D. Contreras, M. Castro, and D. S. de la Torre, "Performance evaluation of Bluetooth low energy in indoor positioning systems," *Trans. Emerg. Telecommun. Technol.*, vol. 28, no. 1, Aug. 2017, Art. no. e2864.

[21] P. Kriz, F. Maly, and T. Kozel, "Improving indoor localization using Bluetooth low energy beacons," *Mobile Inf. Syst.*, vol. 2016, pp. 1–11, Mar. 2016.

[22] A. De Angelis *et al*, "Design and characterization of a portable ultrasonic indoor 3-D positioning system," *IEEE Trans. Instrum. Meas.*, vol. 64, no. 10, pp. 2616–2625, May 2015.

[23] A. Mulloni, D. Wagner, I. Barakonyi, and D. Schmalstieg, "Indoor positioning and navigation with camera phones," *IEEE Pervasive Comput.*, vol. 8, no. 2, pp. 22–31, 1st Quart., 2009.

[24] Y. Gu, A. Lo, and I. Niemegeers, "A survey of indoor positioning systems for wireless personal networks," *IEEE Commun. Surveys Tuts.*, vol. 11, no. 1, pp. 13–32, Mar. 2009.

[25] F. Zhao, T. Huang, and D. Wang, "A probabilistic approach for WiFi fingerprint localization in severely dynamic indoor environments," *IEEE Access*, vol. 7, pp. 116348–116357, 2019.

[26] J. C. Torrado, G. Montoro, and J. Gomez, "Easing the integration: A feasible indoor way finding system for cognitive impaired people," *Pervasive Mobile Comput.*, vol. 31, pp. 137–146, Sep. 2016.

[27] R. Ma, Q. Guo, C. Hu, and J. Xue, "An improved WiFi indoor positioning algorithm by weighted fusion," *Sensors*, vol. 15, no. 9, pp. 21824–21843, Aug. 2015.

[28] Z. Zheng *et al.*, "Weight-RSS: A calibration-free and robust method for WLAN-based indoor positioning," *Int. J. Distrib. Sens. Netw.*, vol. 11, no. 4, Apr. 2015, Art. no. 573582.

[29] L.-F. Shi, Y. Wang, G.-X. Liu, S. Chen, Y.-L. Zhao, and Y.-F. Shi, "A fusion algorithm of indoor positioning based on PDR and RSS fingerprint," *IEEE Sens. J.*, vol. 18, no. 23, pp. 9691–9698, Oct. 2018.

[30] G. Caso and L. De Nardis, "Virtual and oriented WiFi fingerprinting indoor positioning based on multi-wall multi-floor propagation models," *Mobile Netw. Appl.*, vol. 22, no. 5, pp. 825–833, Jul. 2017.

[31] S. Kim, H. Cho, J. M. Gil, and J. Park, "Method of indoor localization using signal indication for the Internet of Things," *Adv. Sci. Lett.*, vol. 22, no. 9, pp. 2296–2299, Sep. 2016.

[32] T. Jure and K. Matjaz, "A self-adaptive model-based Wi-Fi indoor localization method," *Sensors*, vol. 16, no. 12, p. 2074, Dec. 2016.

[33] D. Li, B. Zhang, and C. Li, "A feature-scaling-based *k*-nearest neighbor algorithm for indoor positioning systems," *IEEE Internet Things J.*, vol. 3, no. 4, pp. 590–597, Oct. 2015.

[34] H. Zou, B. Huang, X. Lu, H. Jiang, and L. Xie, "A robust indoor positioning system based on the procrustes analysis and weighted extreme learning machine," *IEEE Trans. Wireless Commun.*, vol. 15, no. 2, pp. 1252–1266, May 2016.

[35] L. Elina and L. Elena, "On the choice of access point selection criterion and other position estimation characteristics for WLAN-based indoor positioning," *Sensors*, vol. 16, no. 5, p. 737, May 2016.

[36] Y. Xia, Z. Zhang, and L. Ma, "Radio map updated method based on subscriber locations in indoor WLAN localization," *J. Syst. Eng. Electron.*, vol. 26, no. 6, pp. 1202–1209, Dec. 2015.

[37] Y. Zhou, X. Chen, S. Zeng, J. Liu, and D. Liang, "AP selection algorithm in WLAN indoor localization," *Inf. Technol. J.*, vol. 12, no. 16, pp. 3773–3776, 2013.

[38] A. Khalajmehrabadi, N. Gatsis, and D. Akopian, "Modern WLAN fingerprinting indoor positioning methods and deployment challenges," *IEEE Commun. Surveys Tuts.*, vol. 19, no. 3, pp. 1974–2002, 3rd Quart., 2017.

[39] J. Li *et al.*, "Indoor localization method based on regional division with IFCM," *Electronics*, vol. 8, no. 5, p. 559, May 2019.

[40] J. C. D. Angeles, E. P. Dadios, "Self-adaptive WLAN access point for optimizing network performance using multi-objective genetic algorithm (MOGA)," *J. Comput. Innov. Eng. Appl.*, vol. 2, no. 1, pp. 40–56, Aug. 2017.

[41] H. Zou, Y. Luo, X. Lu, H. Jiang, and L. Xie, "A mutual information based online access point selection strategy for WiFi indoor localization," in *Proc. IEEE Int. Conf. Auto. Sci. Eng. (CASE)*, 2015, pp. 180–185.

[42] Y. Chen, Q. Yang, J. Yin, and Q. Yang, "Power-efficient access-point selection for indoor location estimation," *IEEE Trans. Knowl. Data Eng.*, vol. 18, no. 7, pp. 877–888, May 2006.

[43] I. Sharp and K. Yu, *Wireless Positioning: Principles and Practice*. Singapore: Springer, 2019, pp. 221–222.

[44] G. Harish, "A hybrid PSO-GA algorithm for constrained optimization problems," *Appl. Math. Comput.*, vol. 274, pp. 292–305, Feb. 2016.

[45] W. Darrell, "A genetic algorithm tutorial," *Stat. Comput.*, vol. 4, no. 2, pp. 65–85, Jun. 1994.

[46] L. Adam and D. Lipowska, "Roulette-wheel selection via stochastic acceptance," *Physica A Stat. Mech. Appl.*, vol. 391, no. 6, pp. 2193–2196, Mar. 2012.
[47] J. Kennedy and R. C. Eberhart, "Particle swarm optimization," in *Proc. IEEE Int. Conf. Neural Netw.*, 1995, pp. 1942–1948.
[48] G. Stimac, S. Braut, and R. Žigulić, "Comparative analysis of PSO algorithms for PID controller tuning," *Chin. J. Mech. Eng.*, vol. 27, no. 5, pp. 928–936, Dec. 2014.
[49] A. Alfi and H. Modares, "System identification and control using adaptive particle swarm optimization," *Appl. Math. Model.*, vol. 35, no. 3, pp. 1210–1221, Mar. 2011.
[50] M. Hamidreza, A. Alfi, and M. B. N. Sistani, "Parameter estimation of bilinear systems based on an adaptive particle swarm optimization," *Eng. Appl. Artif. Intell.*, vol. 23, no. 7, pp. 1105–1111, Oct. 2010.
[51] W. Zhang, X. Hua, K. Yu, W. Qiu, S. Zhang, and X. He, "A novel WiFi indoor positioning strategy based on weighted squared Euclidean distance and local principal gradient direction," *Sens. Rev.*, vol. 39, no. 1, pp. 99–106, Jan. 2019.
[52] Q. Wang, Y. Feng, X. Zhang, Y. Sun, and X. Lu, "IWKNN: An effective Bluetooth positioning method based on Isomap and WKNN," *Mobile Inf. Syst.*, vol. 2016, pp. 1–11, Sep. 2016.
[53] P. A. Karegar, "Wireless fingerprinting indoor positioning using affinity propagation clustering methods," *Wireless Netw.*, vol. 24, no. 8, pp. 2825–2833, Apr. 2017.
[54] J. Hu, D. Liu, Z. Yan, and H. Liu, "Experimental analysis on weight *K*-nearest neighbor indoor fingerprint positioning," *IEEE Internet Things J.*, vol. 6, no. 1, pp. 891–897, Feb. 2019.

Wei Zhang (Member, IEEE) received the Ph.D. degree from the School of Geodesy and Geomatics, Wuhan University, Wuhan, China, in 2018.

He is currently a Postdoctoral Researcher with the Department of Research Institute for Smart Cities, Shenzhen University, Shenzhen, China. His current research focuses on the indoor positioning and indoor navigation.

Kegen Yu (Senior Member, IEEE) received the Ph.D. degree in electrical engineering from the University of Sydney, Sydney, NSW, Australia, in 2003.

He was with Jiangxi Geological and Mineral Bureau, Nanchang, China; Nanchang University, Nanchang; the University of Oulu, Oulu, Finland; CSIRO ICT Center, Sydney; Macquarie University, Sydney; the University of New South Wales, Sydney; and Wuhan University, Wuhan, China. He is currently a Professor with the School of Environmental Science and Spatial Informatics, China University of Mining and Technology, Xuzhou, China. His research interests include global-navigation-satellite-system reflectometry, ground-based and satellite-based positioning, and remote sensing.

Weixi Wang received the Ph.D. degree in geodesy and survey engineering from Liaoning Technical University, Liaoning, China, in 2007.

He completed Postdoctoral Fellowship with the School of Resource and Environmental Sciences, Wuhan University, Wuhan, China, in 2013. He has authored or coauthored over 30 refereed journal and conference papers, and one book. He is currently an Associate Professor with the School of Architecture and Urban Planning, Shenzhen University, Shenzhen, China, where he is the Deputy Head of the Department of Urban Spatial Information Engineering. His current research interests include real-time positioning and navigation, target feature extraction and matching, and 3-D model reconstruction.

Xiaoming Li (Member, IEEE) received the Ph.D. degree in photogrammetry and remote sensing from Wuhan University, Wuhan, China, in 2011.

He is currently an Associate Professor with the School of Architecture and Urban Planning, Shenzhen University, Shenzhen, China. His current research interests include real-time positioning and navigation, target feature extraction and matching, and 3-D model reconstruction.